

Effect of Biopipe Total Flowrate on Venturi Aerator Performance

Hayder M. Jasem^{1,2,*}, Kifah M. Khudair³

^{1,3} Department of Civil Engineering, College of Engineering, University of Basrah, Basrah, Iraq

² Department of Structures and Water Resources, College of Engineering, University of Kufa, Najaf, Iraq

E-mail addresses: hayderm.almosawey@uokufa.edu.iq, kifah.khudair@uobasrah.edu.iq

Received: 26 June 2022; Accepted: 21 September 2022; Published: 2 July 2023

Abstract

There is a vacuum created when water goes past a pipe constriction. Air may be pulled into the main flow by drilling a hole in the pipe near where the vacuum happens. Venturi aerator is an example of the application in action. A vacuum is formed at the suction holes of the Venturi tube when there is a small difference in pressure between the input and output sides. To demonstrate the link between total flow rate and Venturi aerator performance, a Venturi aerator (model 1584) was introduced at a specific point in a Biopipe system. For this purpose, a physical model on a pilot scale was constructed and installed in an existing sewage treatment plant. Dissolved oxygen concentrations were measured at four locations along the Biopipe at different values of wastewater flowrates. The study results showed that raising the total flow rate increased the amount of air injected by the Venturi aerator. When the total flow rate was less than 4 m³/hour, the Venturi aerator stops sucking air and produces negative consequences.

Keywords: Vacuum, Venturi aerator, Biopipe system, Performance.

© 2023 The Authors. Published by the University of Basrah. Open-access article.

<https://doi.org/10.33971/bjes.23.1.1>

1. Introduction

As the number of people on the earth grows every year, the need for clean water is rising quickly. People are now more aware that climate changes and urbanization are likely to cause less rain in many parts of the world [1]. The problem of managing water quality has a big impact on how river basins are planned and how water pollution is stopped. In the last few decades, the need to keep an eye on the water quality of many rivers by taking the same measurements of different water quality variables has changed [2].

Water's ecological quality is heavily reliant on its oxygen content. The better the water system, the greater the concentration of dissolved oxygen must be. Dissolved oxygen (DO) is a key indicator of water quality and ecosystem health. Air bubbles entrain oxygen into water. Air bubble entrainment is used in many industrial and environmental operations to aerate a liquid [3]. Water aeration is often used to enhance the quality of lakes and rivers by increasing the concentration of DO. In aeration, tiny bubbles of air are introduced into a stream and allowed to ascend through the water column. When there is a shortage of dissolved oxygen in the system, aeration aids in its replenishment. DO levels may be raised by introducing a variety of hydraulic devices that shake up the water and create air bubbles. Wastewater treatment facilities are estimated to use around 4 % of the nation's total energy consumption [4]. Over 60 % of the total energy utilized in wastewater treatment facilities is used in aeration operations [5].

More and more hydraulic and environmental engineers are discovering the benefits of the relatively new Venturi aeration method, which has seen an increase in interest recently [6]. Venturi aeration is one of the best methods for increasing water body oxygen content and air entrainment. Vacuum (air

suction) develops at the venturi tube suction holes when the input and output sides of the venturi tube have a small difference in pressure as shown in Fig. 1. High-velocity jet streams are formed when pressurized operational (motive) fluids (such as wastewater or water), reach the Venturi tube entrance. The drop in pressure in the throat part of the venturi tube is caused by an increase in velocity in the throat segment due to the differential pressure. This pressure decrease allows for air to be pushed via the suction ports and dynamically absorbed into the primary stream. Pressure energy is transformed back into kinetic energy as the jet stream diffuses near the venturi tube exit (but at a level lower than the venturi tube inlet pressure). Venturi tubes are very efficient, needing a difference of less than 20 percent to commence suction.

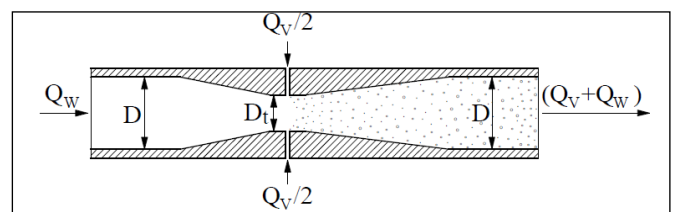


Fig. 1 Venturi tube induced air suction [3].

There are several benefits of using Venturi tubes into water aeration systems. The Venturi tube requires no external power to function. It has no moving components, which boosts its durability and reduces the likelihood of collapse. It's common for the Venturi tube to be made of plastic, which is resistant to a variety of chemicals. Maintenance and operator attentions are low with this device. Simple in design, it's inexpensive in comparison to other devices with comparable capabilities. Almost any new or existing system can be made to work with

this as long as there is enough pressure in the system to provide the necessary pressure difference. There are no large concentrations of material in the Venturi tube since it uses a vacuum principle instead of a pressure concept. There is less risk of caustic chemicals being released into the atmosphere via cracks or fractures in the pipe.

2. Venturi tube air injection technique

Diverging tubes convert velocity heads to pressure heads, whereas converging tubes convert pressure heads to velocity heads. The two can be joined to create a venturi tube, named for the Italian scientist who discovered its concept in 1791 [3]. As seen in Fig. 2, it comprises a tube with a narrower throat that results in a rise in velocity and a decrease in pressure, followed by a progressively diverging section where the velocity is converted back into pressure with little frictional loss.

Points 1 and 2 are located before and at the contraction of the Venturi tube, see Fig. 2, are used to write the Bernoulli equation, and in case of ideal liquid, it can be written as:

$$\frac{p_1}{\gamma} + z_1 + \frac{V_1^2}{2g} = \frac{p_2}{\gamma} + z_2 + \frac{V_2^2}{2g} \quad (1)$$

Where, p is the pressure (kPa), γ is the specific weight (kN/m³), z is the elevation (m), V is the flow velocity (m/sec), g is the gravity acceleration (m/sec²), and the subscripts 1 and 2 indicate the first and second points, respectively.

Since z_1 equals z_2 , Equation (1) may indeed be written as follows:

$$\frac{p_2}{\gamma} = \frac{p_1}{\gamma} + \frac{V_1^2}{2g} - \frac{V_2^2}{2g} \quad (2)$$

We can define the flow rate at point 1 as a function of the flow rate at point 2 and the ratio of the two flow regions by using the continuity equation at points 1 and 2.

$$V_1 = \left(\frac{A_2}{A_1}\right) V_2 = \beta V_2 \quad (3)$$

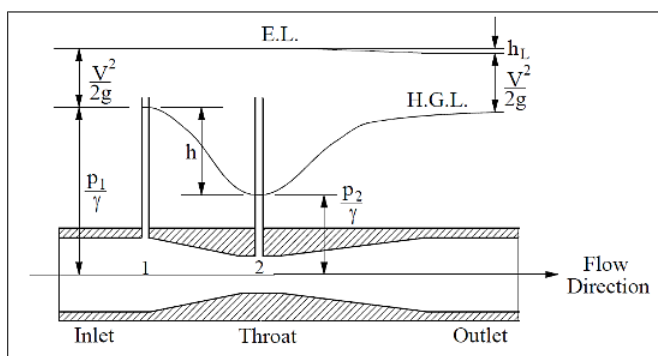


Fig. 2 Venturi tube explanation diagram [7].

where A_1 and A_2 represent the flow areas at locations of points 1 and 2, respectively, and A_2/A_1 represents the ratio of the Venturi tube's throat flow area to its entrance flow area. Equation (2) may be solved by substituting β value.

$$\frac{p_2}{\gamma} = \frac{p_1}{\gamma} + \frac{V_2^2 (\beta^2 - 1)}{2g} \quad (4)$$

The venturi impact occurs as a result of a decrease in throat pressure as throat velocity rises. As a consequence of the differential pressure, the increase in velocity V_2 through the throat of the Venturi tunnel causes a reduction in pressure p_2 in the throat. Air is dynamically entrained into the motive stream when the pressure p_2 in the throat region decreases below the atmospheric pressure.

3. Literature review

Using inclined plunging water jets, Bagatur et al. (2002) [8] tested the influence of nozzle shape on air entrainment rate and oxygen transfer efficiency and came up with promising results. Baylar et al. (2003) [9] studied the air - entraining rate and oxygen conversion efficiency of the convergent divergent passage of the Venturi nozzle with ventilation holes along its length and in particular the impact of altering the number, location, and open/close state of the air holes. Bagatur and Sekerdag (2003) [10] studied the air - entraining rate of circle nozzles with and without air vents, and in particular, the influence of various numbers and placements of the air holes and the distance between air hole sites and the nozzle outlet. Ozkan et al. (2006) [11] performed a series of laboratory experiments on tap water for studying the efficiency of air injection using Venturi aerator considering the effects of many parameters such as; the dimensions of Venturi aerator and the pipe at which it is installed, and liquid density and viscosity on air injection rate. Zhu et al. (2007) [12] investigated the air entrainment properties in a descending water jet setup with rectangular nozzles and rounded ends. Zhu et al. (2007) [13] applied Venturi aerator to aerate the lagoon of fish's production and investigated the possibility of increasing its aeration efficiency by connecting more than one injector and examined two connection orientations; in parallel and in series. Khound et al. (2017) [14] investigated, experimentally, the efficiency of Venturi aerator as an air supply device in its relation to the hole diameter and location (from the start of the throat section) under different flow conditions (three values of flow rates). Bagatur et al. (2018) [15] conducted an experimental study using tap water to evaluate the performance of different configurations of Venturi aerators. The configurations differed in the number of inlet and outlet pipes.

From the literature review presented above, it can be shown the impact of wastewater flowrate on air injection using a Venturi aerator has not been considered in the previous available studies which highlight the necessity of performing the present study.

4. Materials and methods

4.1. Description of the biopipe physical model

For the study's main objective, a physical model for the Biopipe system was designed. With the help of the physical model, it is possible to determine the amount of dissolved oxygen in wastewater flowing in the Biopipe according to total flowrate of wastewater. The physical model was built in the form of a pilot plant, which will be used for the practical implementation of Venturi aerator. As seen in Fig. 3, the physical model is comprised of a DC electric motor linked to two centrifugal pumps, a storage tank, a sedimentation tank, PVC pipes, flow meters, and a pressure gauge. It also includes four taps which were used as sampling points and gate valves for controlling wastewater flowrate.

Both the sedimentation tank and the storage tank have a capacity of 1 m³. The pumping of wastewater was maintained by the alternative operation of two provided pumps. The two pumps work in succession, one after the other. The pressure and flowrate of wastewater were adjusted by the flow meters and the pressure gauge, respectively. A Venturi aerator was installed at the beginning of the system for the intent of air supply.

Wastewater samples were collected from the four sampling points in order to monitor the DO concentrations along the Biopipe. The DO concentration was measured by using a calibrated portable DO meter type B.C OD 125.2. The wastewater samples were withdrawn at regular intervals at various values of total flowrate. The properties of influent wastewater during the operation time of the pilot plant were; COD is 403 mg/l, TSS is 342 mg/l, pH is 6.94, and NH₃-N is 17.3 mg/l.

4.2. Construction of biopipe physical model

The physical model was constructed and installed at the AL-Baraki Wastewater Treatment Plant in Kufa City, Najaf Governorate, Iraq. The physical model was installed on this site in order to maintain the pilot plant's operation by providing a continuous supply of wastewater. Fig. 4 shows photos of the model at its installation site.

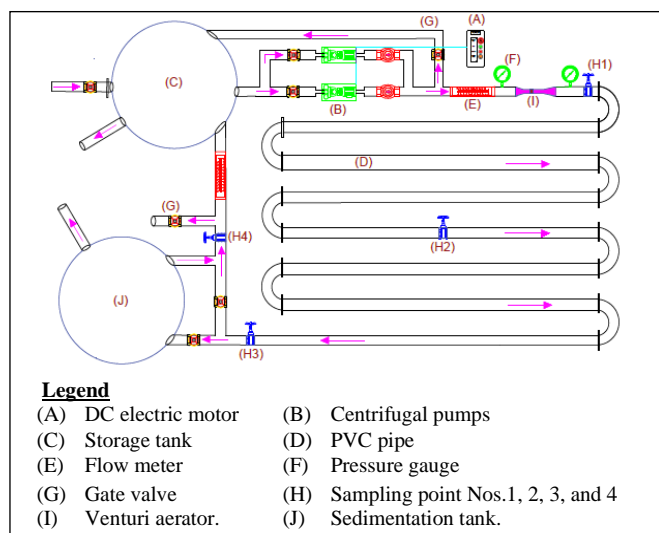


Fig. 3 Schematic diagram of Biopipe physical model.



Fig. 4 Photos of the Biopipe physical model.

4.3. Venturi model selection

Selecting the right model of Venturi aerator is necessary to match the hydraulic conditions and at the same time to supply the required DO. The four criteria permit the selection of any air injector model are; inlet pressure, motive flow rate, outlet pressure, and injection rate [16]. Based on this restriction, Venturi aerator (model 1584) was chosen. Fig. 5 depicts the primary component and dimension of this aerator.

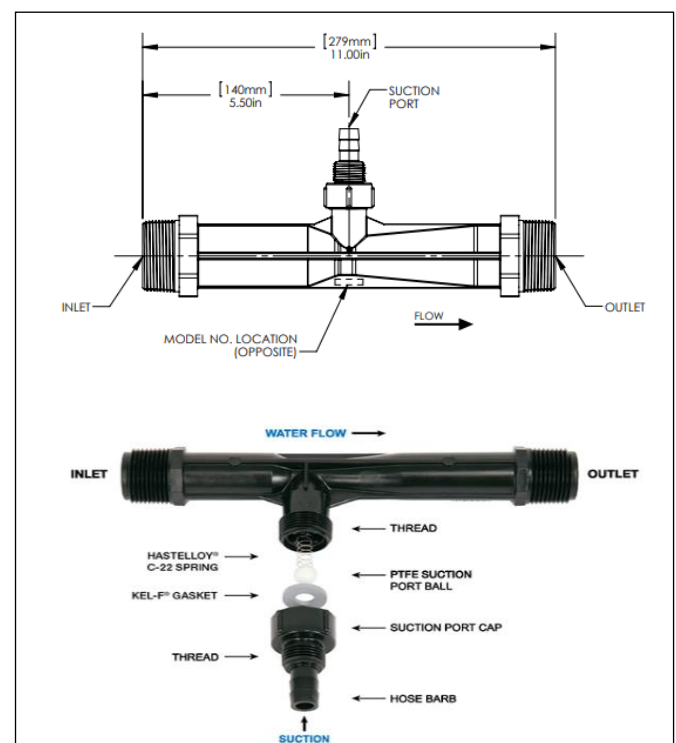
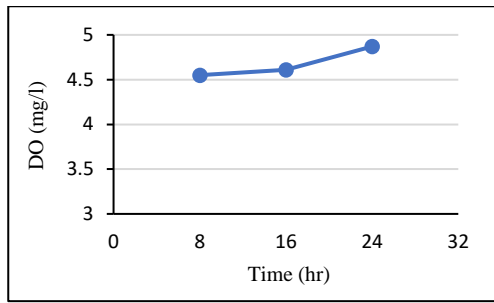


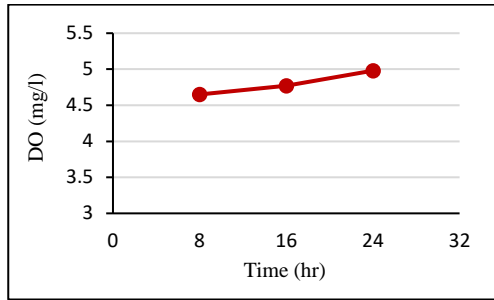
Fig. 5 Specifications of Venturi aerator (model 1584) [16].

5. Results and discussion

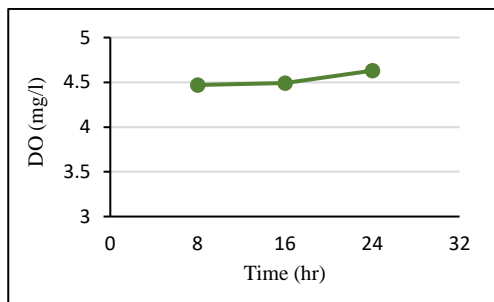
The availability of adequate dissolved oxygen (DO) is a significant indicator of water quality and is necessary for aerobic biological waste water treatment. The first experiment was conducted on January 10, 2021 by stabilizing the wastewater total flow rate at 5 m³/hour and then measuring the DO at the four sampling points every 8 hours. The temporal variation of DO is shown in Fig. 6.



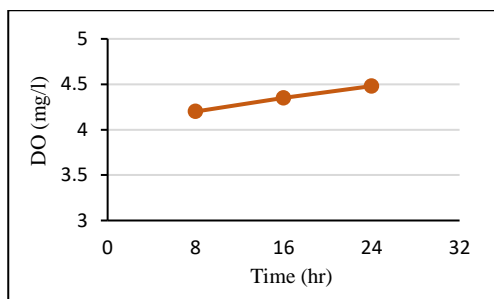
(a) Sampling point No. 1.



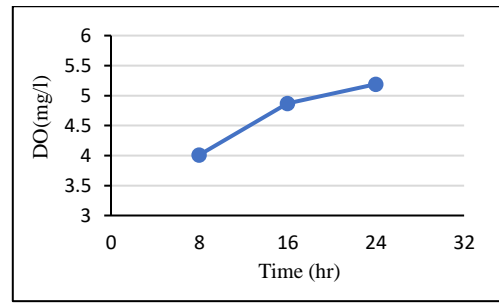
(b) Sampling point No. 2.



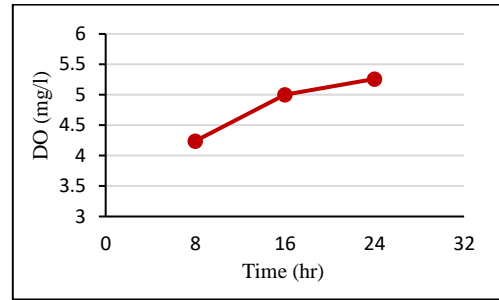
(c) Sampling point No. 3.



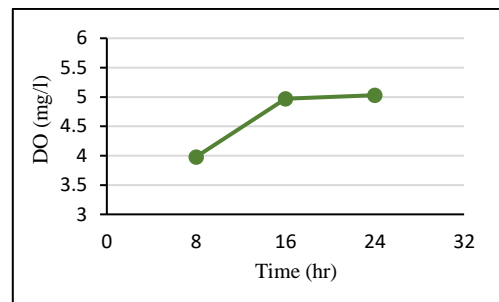
(d) Sampling point No. 4.



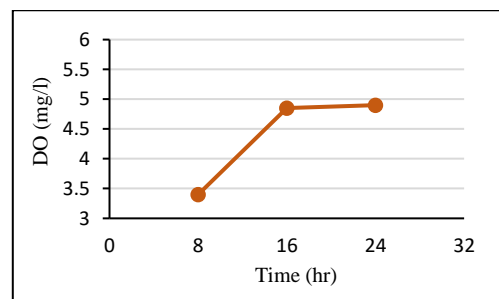
(a) Sampling point No.1.



(b) Sampling point No. 2.



(c) Sampling point No. 3.



(d) Sampling point No. 4.

Fig. 6 DO variation with time at the locations of the four sampling points for total flowrate of wastewater equals $5 \text{ m}^3/\text{hour}$.

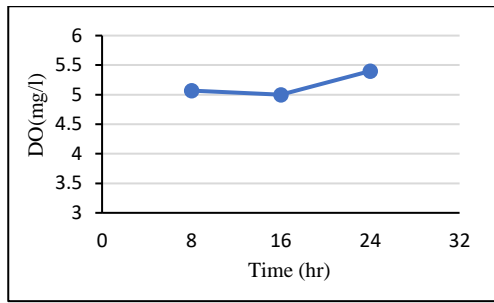
Fig. 6 shows that the DO concentration increases as the running time increases, and the maximum values are reached after 24 hours of plant operation. After 24 operation hours, the highest DO concentration was at sampling point No.2 which equals 4.98 mg/l . The figure shows, also, that there is a jump in the value of the DO concentration at all the locations of sampling points at the 8th hour of plant operation, followed by a slight rise in the DO concentrations beyond this hour.

A second experiment was conducted by raising the overall flow rate to $8 \text{ m}^3/\text{hour}$ and measuring the DO at all the sampling points and the results are shown in Fig. 7. During the first 8 hours of plant operation, the DO values were somewhat lower than those observed in the first experiment, but beyond this period, the DO concentrations were greater than those in the first experiment. The maximum value of DO was 5.26 mg/l and sampling point No. 2.

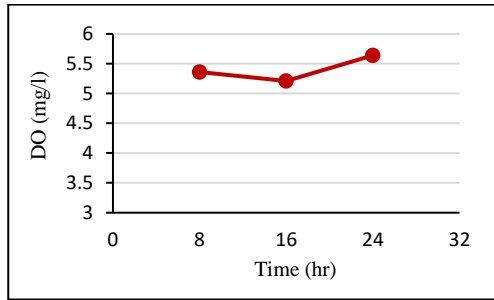
Fig. 7 DO variation with time at the locations of the four sampling points for total flowrate of wastewater equals $8 \text{ m}^3/\text{hour}$.

The total flow rate was raised to $9 \text{ m}^3/\text{hour}$ in the third experiment, and the concentration of DO was measured at each sampling point. The measured DO concentrations in this experiment were higher than those in the first two experiments. Herein, the maximal DO was measured at locations No. 2 and 3 which were 5.64 and 5.75 mg/l , respectively.

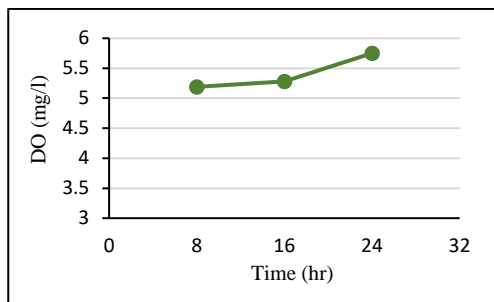
To show the distribution of DO along the entire length of the Biopipe system, the measured values were consistently gathered in Fig. 9 after 24 hours of plant operation. Fig. 9 shows that when the system's total flowrate was increased to its maximum value, the DO reached its highest levels. Maximum DO values were observed at sampling point No. 3 and at the maximum total flow rate ($9 \text{ m}^3/\text{hour}$).



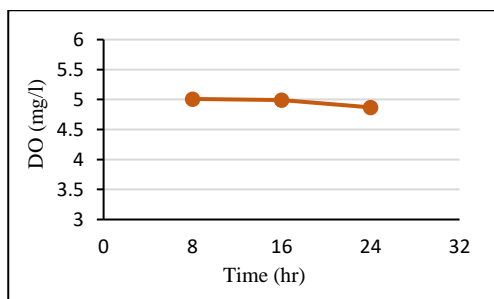
(a) Sampling point No. 1.



(b) Sampling point No. 2.



(c) Sampling point No. 3.



(d) Sampling point No. 4.

Fig. 8 DO variation with time at the locations of the four sampling points for total flowrate of wastewater equals $9 \text{ m}^3/\text{hour}$.

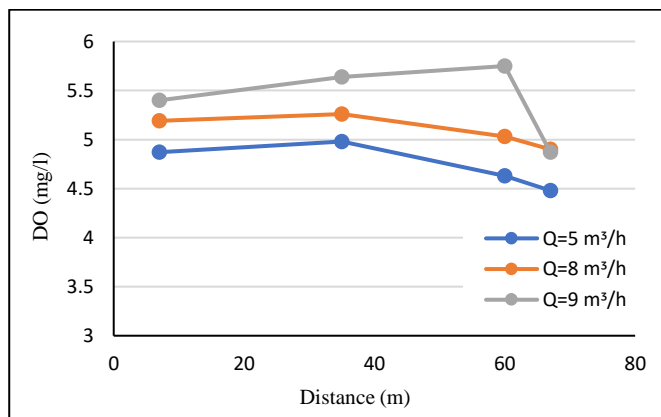


Fig. 9 DO concentration distribution along the Biopipe for different total flowrate values.

6. Conclusions

The main outcomes of this study include:

1. The concentration of DO increases with the increase of operation time. The first eight hours of trials and for all flow rate values, a significant rise in DO concentration values was found; however, beyond this period, the increase becomes minimal.
2. The DO increases with the increase of total flowrate. When the total discharge was $9 \text{ m}^3/\text{hour}$, the greatest value of DO was obtained which was 5.75 mg/l .
3. The value of the DO increased with the distance along the Biopipe until the mid-span was reached. After that point, the DO concentration slightly decreased over the remaining length of the pipes.
4. When the total flowrate reached a value of $4 \text{ m}^3/\text{hour}$, Venturi aerator model (1584) ceased to inject air into the Biopipe.

References

- [1] H. T. Ibrahim, H. Qiang., and W. S. Al-Rekabi, "Simultaneous organics and nutrients removal from domestic wastewater in a combined cylindrical anoxic/aerobic moving bed biofilm reactor", *Research Journal of Applied Sciences, Engineering and Technology*, Vol. 7, Issue 9, pp. 1887-1895, 2014. <https://doi.org/10.19026/rjaset.7.478>
- [2] A. S. Dawood, H. K. Hussain, and A. A. Hassan, "Modeling of river water quality parameters using artificial neural network - A case study", *International Journal of Advances in Mechanical and Civil Engineering*, Vol. 3, Issue 5, pp. 51-56, 2016.
- [3] A. Baylar, M. C. Aydin, M. Unsal, and F. Ozkan, "Numerical modeling of Venturi flows for determining air injection rates using Fluent V6.2", *Mathematical and Computational Applications*, Vol. 14, Issue 2, pp. 97-108, 2009. <https://doi.org/10.3390/mca14020097>
- [4] Z. Zhang and Y. Zeng, "A minimizing pump energy in a wastewater processing plant", *Energy*, Vol. 47, Issue 1, pp. 505-514, 2012. <https://doi.org/10.1016/j.energy.2012.08.048>
- [5] M. Brandt, R. Middleton, G. Wheale, and F. Schulting "Energy efficiency in the water industry", *A Global Research Project, Water Practical Technology*, Vol. 6, Issue 2, 2011. <https://doi.org/10.2166/wpt.2011.028>
- [6] R. Mahmud, M. Erguvan, and D. Macphee, "Performance of closed loop Venturi aspirated aeration system: Experimental study and numerical analysis with discrete bubble model", *MDPI, Water*, Vol. 12, Issue 6, 2020. <https://doi.org/10.3390/w12061637>
- [7] R. L. Daugherty, J. B. Franzini, and E. J. Finnemore, *Fluid Mechanics with Engineering Applications*, McGraw-Hill Inc., New York, 1985.
- [8] T. Bagatur, A. Baylar, and N. Sekerdag, "The effect of nozzle type on air entrainment by plunging water jets", *Water Quality Research Journal*, Vol. 37, Issue 3, pp. 599-612, 2002. <https://doi.org/10.2166/wqrj.2002.040>
- [9] A. Baylar. and M. E. Emiroglu, "Air entrainment and oxygen transfer in a Venturi", *Proceedings of the Institution of Civil Engineers, Water and Maritime Engineering*, Vol. 156, Issue 3, pp. 249-255, 2003. <https://doi.org/10.1680/wame.2003.156.3.249>

- [10] T. Bagatur and N. Sekerdag, "Air-entrainment characteristics in a plunging water jet system using rectangular nozzles with rounded ends", *Water SA*, Vol. 29, Issue 1, pp. 35-38, 2003.
<https://doi.org/10.4314/wsa.v29i1.4943>
- [11] H. Zhu, T. Imai, K. Tani, M. Ukita, M. Sekine, T. Higuchi, and Z. Zhang, "Improvement of oxygen transfer efficiency in aerated ponds using liquid-film-assisted approach", *Water Science and Technology*, Vol. 55, Issue 11, pp.183-191, 2007. <https://doi.org/10.2166/wst.2007.353>
- [12] F. Ozkan, M. Ozturk, and A. Baylar, "Experimental investigations of air and liquid injection by Venturi tubes", *Water and Environment Journal*, Vol. 20, Issue 3, pp. 114-122, 2006.
<https://doi.org/10.1111/j.1747-6593.2005.00003.x>
- [13] J. Zhu, C. F. Miller, C. Dong, X. Wu, L. Wang, and S. Mukhtar, "Aerator module development using Venturi air injectors to improve aeration efficiency", *Applied Engineering in Agriculture*, Vol. 23, Issue 5, pp. 661-667, 2007.
- [14] K. Amarjyoti, Y. Anamika, S. Sudipto, and K. Avinash, "Influence of throat length and flow parameters on a Venturi as an aerator", *International Journal of Agriculture, Environment and Biotechnology, IJAEB*, Vol. 10, Issue 6, pp. 717-723, 2017.
<https://doi.org/10.5958/2230-732X.2017.00089.4>
- [15] T. Bagatur, F. Onen, and N. Kayaalp, "Testing of system performance for different aerator configurations using Venturi", *El-Cezerî Journal of Science and Engineering*, Vol. 5, Issue 3, pp. 724-733, 2018.
<https://doi.org/10.31202/ecjse.402032>
- [16] Mazzi Injector Company, LLC, 500 Rooster Drive, Bakersfield, CA 93307-9555 USA, 2016.